AMERICAN SOCIETY FOR MICROBIOLOGY | Journal of Virology®

VIRUS-CELL INTERACTIONS

Mutations in the Spike Protein of Middle East Respiratory Syndrome Coronavirus Transmitted in Korea Increase Resistance to Antibody-Mediated Neutralization

Hannah Kleine-Weber,[a,b] Mahmoud Tarek Elzayat,[a] Lingshu Wang,[c] Barney S. Graham,[c] Marcel A. Müller,[d,e] Christian Drosten,[d,e] Stefan Pöhlmann,[a,b] Markus Hoffmann[a]

[a]Infection Biology Unit, German Primate Center, Göttingen, Germany
[b]Faculty of Biology and Psychology, University of Göttingen, Göttingen, Germany
[c]Vaccine Research Center, National Institute of Allergy and Infectious Diseases, National Institutes of Health, Bethesda, Maryland, USA
[d]Institute of Virology, Charité-Universitätsmedizin Berlin, Berlin, Germany
[e]German Centre for Infection Research, associated partner Charité, Berlin, Germany

ABSTRACT Middle East respiratory syndrome coronavirus (MERS-CoV) poses a threat to public health. The virus is endemic in the Middle East but can be transmitted to other countries by travel activity. The introduction of MERS-CoV into the Republic of Korea by an infected traveler resulted in a hospital outbreak of MERS that entailed 186 cases and 38 deaths. The MERS-CoV spike (S) protein binds to the cellular protein DPP4 via its receptor binding domain (RBD) and mediates viral entry into target cells. During the MERS outbreak in Korea, emergence and spread of viral variants that harbored mutations in the RBD, D510G and I529T, was observed. Counterintuitively, these mutations were found to reduce DPP4 binding and viral entry into target cells. In this study, we investigated whether they also exerted proviral effects. We confirm that changes D510G and I529T reduce S protein binding to DPP4 but show that this reduction only translates into diminished viral entry when expression of DPP4 on target cells is low. Neither mutation modulated S protein binding to sialic acids, S protein activation by host cell proteases, or inhibition of S protein-driven entry by interferon-induced transmembrane proteins. In contrast, changes D510G and I529T increased resistance of S protein-driven entry to neutralization by monoclonal antibodies and sera from MERS patients. These findings indicate that MERS-CoV variants with reduced neutralization sensitivity were transmitted during the Korean outbreak and that the responsible mutations were compatible with robust infection of cells expressing high levels of DPP4.

IMPORTANCE MERS-CoV has pandemic potential, and it is important to identify mutations in viral proteins that might augment viral spread. In the course of a large hospital outbreak of MERS in the Republic of Korea in 2015, the spread of a viral variant that contained mutations in the viral spike protein was observed. These mutations were found to reduce receptor binding and viral infectivity. However, it remained unclear whether they also exerted proviral effects. We demonstrate that these mutations reduce sensitivity to antibody-mediated neutralization and are compatible with robust infection of target cells expressing large amounts of the viral receptor DPP4.

KEYWORDS MERS, antibody, neutralization, spike, virus entry

The family *Coronaviridae* harbors enveloped, positive-sense RNA viruses that infect mammals and birds (1). Several coronaviruses (CoV) within the genera *Alphacoronavirus* and *Betacoronavirus* constantly circulate in the human population and cause

Citation Kleine-Weber H, Elzayat MT, Wang L, Graham BS, Müller MA, Drosten C, Pöhlmann S, Hoffmann M. 2019. Mutations in the spike protein of Middle East respiratory syndrome coronavirus transmitted in Korea increase resistance to antibody-mediated neutralization. J Virol 93:e01381-18. https://doi.org/10.1128/JVI.01381-18.

Editor Tom Gallagher, Loyola University Medical Center

Address correspondence to Stefan Pöhlmann, spoehlmann@dpz.eu, or Markus Hoffmann, mhoffmann@dpz.eu.

Received 10 August 2018
Accepted 25 October 2018
Accepted manuscript posted online 7 November 2018
Published 4 January 2019

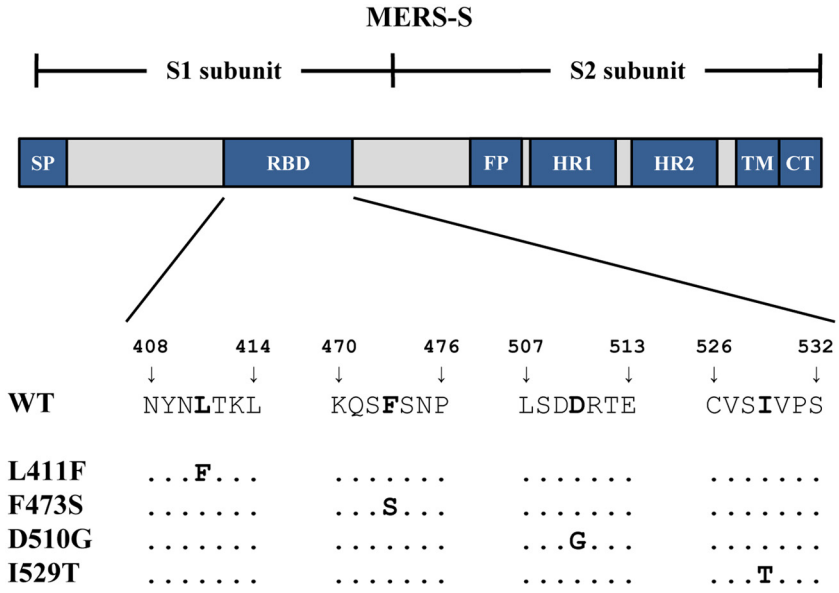

FIG 1 Schematic illustration of the MERS-CoV spike glycoprotein and location of the receptor binding domain (RBD) polymorphisms. The MERS-CoV spike glycoprotein (MERS-S) consists of two subunits (S1 and S2). The S1 subunit contains an N-terminal signal peptide (SP) and an RBD, which binds to the receptor DPP4. The S2 subunit harbors the functional elements required for membrane fusion, a fusion peptide (FP), and two heptad repeats (HR1 and HR2), as well as the transmembrane domain (TD) and a cytoplasmic tail (CT). Below the scheme, the locations of the four amino acid polymorphisms investigated in this study (L411F, F473S, D510G, and I529T) are highlighted (bold letters).

mild respiratory disease. In addition, the betacoronaviruses severe acute respiratory syndrome (SARS)- and Middle East respiratory syndrome (MERS)-CoV can be zoonotically transmitted from animals to humans (1). Camels serve as a natural reservoir for MERS-CoV, and infected animals may exhibit mild respiratory symptoms (2, 3). In contrast, transmission of MERS-CoV to humans induces fatal disease in about 36% of the afflicted patients (4). Most MERS cases have been documented in the Middle East, but the virus has been introduced into several other countries due to international travel. At present, human-to-human transmission of MERS-CoV is inefficient. However, massive MERS outbreaks have been observed in hospital settings (5). For instance, the introduction of MERS-CoV into the Republic of Korea by a single infected traveler in 2015 resulted in 186 infections, including secondary, tertiary, and quaternary cases, and 38 deaths (6, 7). Whether the virus responsible for the Korean outbreak harbored mutations that promoted human to human spread is incompletely understood.

The infectious entry of MERS-CoV into target cells is mediated by the viral spike glycoprotein (MERS-S), which is incorporated into the viral envelope. MERS-S contains a surface unit, S1, and a transmembrane unit, S2. The S1 subunit binds to the main receptor, DPP4/CD26 (8), and the secondary receptor, sialic acids (9), while the S2 subunit facilitates fusion of the viral envelope with a cellular membrane. Membrane fusion depends on prior proteolytic cleavage (activation) of the inactive S protein precursor, S0, by host cell proteases. Specifically, the endosomal cysteine protease cathepsin L (CatL) and the type II transmembrane serine protease, TMPRSS2, located at the plasma membrane can activate MERS-S (10–12). Sequence analysis revealed that MERS-CoV variants observed during the Korean outbreak contained polymorphisms D510G and I529T and that the respective viral variants were transmitted to other patients (13, 14). The D510G and I529T polymorphisms are located in the receptor binding domain (RBD) (Fig. 1), a portion of S1 that is required for binding to DPP4, and one can speculate that they might increase viral fitness and/or transmissibility. However, counterintuitively, both D510G and I529T were shown to decrease binding to DPP4 and I529T was shown to decrease MERS-S-driven entry into cells (14), and it is at present unknown whether the virus benefits from these changes.

Here we show that several parameters controlling efficiency of MERS-S-driven entry, including sialic acid engagement and blockade by interferon (IFN)-induced transmembrane proteins (IFITMs), are not modulated by D510G and I529T. Moreover, we confirm that D510G and I529T reduce DPP4 binding but show that this translates into reduced entry only when small amounts of DPP4 are expressed. Finally, we demonstrate that D510G and I529T reduce sensitivity to antibody-mediated neutralization, suggesting that these mutations might not alter viral transmissibility but might increase viral spread in infected patients in the presence of an antibody response.

RESULTS

Polymorphisms D510G and I529T in MERS-S of Korean patients reduce DPP4 binding but allow efficient entry into cells expressing large amounts of DPP4. We first investigated whether polymorphisms identified during the Korean MERS outbreak, D510G and I529T (13, 14) (Fig. 1), are compatible with robust S protein expression and S protein-driven host cell entry. For comparison, we analyzed polymorphisms found in MERS-S from viruses from the Arabian Peninsula, L411F and F473S (15–19) (Fig. 1); these changes had previously not been investigated for their impact on MERS-S-driven entry. For our analyses of MERS-S-mediated entry, we employed a previously described vesicular stomatitis virus (VSV)-based pseudotyping system (20), which faithfully mimics central aspects of MERS-CoV entry into target cells (21).

Analysis of 293T cells transfected to express the S proteins under study followed by immunoblot and signal quantification revealed that wild-type (WT) MERS-S and all S protein variants were comparably expressed (Fig. 2A). Similarly, all S proteins were proteolytically processed (Fig. 2A, top), in agreement with the finding that furin processes the S protein in MERS-S-transfected and MERS-CoV-infected cells. Finally, all S protein mutants were efficiently incorporated into VSV particles, although incorporation of mutant F473S was slightly reduced compared to that of MERS-S WT (Fig. 2B). Thus, the polymorphisms studied did not impact S protein expression, proteolytic processing, or, with the exception of mutant F473S, incorporation into VSV particles.

Next we analyzed whether the polymorphisms impacted entry into the colon-derived cell line Caco-2, the African green monkey kidney cell line Vero E6, and the human adrenal gland-derived cell line 293T (either control transfected or transfected with DPP4 expression plasmid [293T + DPP4]). These cell lines were chosen for analysis because they are permissive to MERS-CoV infection and were previously used to study host cell interactions of MERS-CoV (22–25). The selected cell lines were highly permissive to transduction by rhabdoviral particles harboring VSV glycoprotein (VSV-G; positive control), while transduction by particles bearing no glycoprotein (negative control) was within background levels, as expected (Fig. 3A). Changes L411F and F473S observed in MERS-CoV from humans and camels in the Middle East had no effect on transduction efficiency. In contrast, changes I529T and, to a lesser degree, D510G observed in Korean MERS patients reduced entry into Vero E6 and 293T cells (Fig. 3A) and diminished binding to DPP4 (Fig. 3B), in agreement with published data (14). However, these mutations had only a modest effect on transduction of Caco-2 and 293T cells expressing saturating amounts of DPP4 (293T + DPP4), respectively (Fig. 3A and data not shown). The finding that directed expression of DPP4 could largely rescue the inhibitory effect of D510G and I529T on transduction of 293T cells prompted us to investigate whether the impact of these changes on S protein-driven entry was dependent on the level of DPP4 expression. Indeed, quantitative reverse transcription-PCR (Fig. 3C) and flow cytometry (Fig. 3D) revealed that Caco-2 and 293T + DPP4 cells, which can be readily transduced by MERS-S D510G and I529T variants, expressed substantially higher levels of DPP4 than 293T and Vero E6 cells, which are not readily susceptible to transduction mediated by S protein mutants D510G and I529T (Fig. 3C and D). Collectively, our results confirm that D510G and I529T reduce S protein binding to DPP4 but also suggest that this reduction translates into diminished S protein-driven cell entry only when DPP4 expression is low.

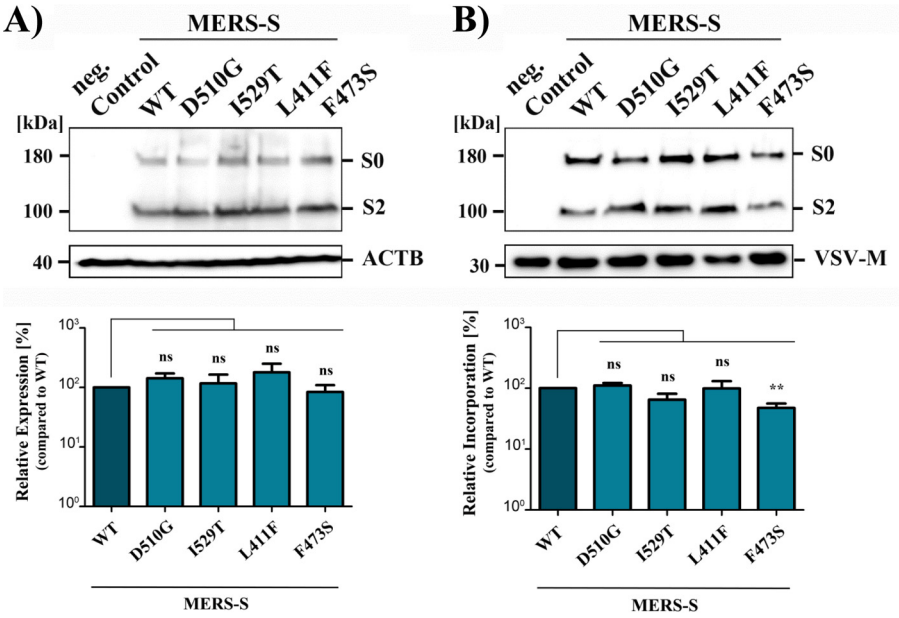

FIG 2 All MERS-S variants analyzed were robustly expressed and incorporated into rhabdoviral particles. (A, top) Expression plasmids for the indicated S proteins or empty plasmid (control) were transfected into 293T cells. Whole-cell lysates (WCL) were prepared from transfected cells, and S protein expression was analyzed by SDS-PAGE and immunoblotting using anti-V5 antibody reactive against the V5 epitope at the C terminus of the S proteins. Detection of β-actin (ACTB) served as a negative control. Similar results were obtained in three separate experiments. (B, top) Expression plasmids for the indicated S proteins or empty plasmid (control) were transfected into 293T cells and the cells were then used to produce rhabdoviral particles. The particles were subsequently pelleted by centrifugation through a sucrose cushion and analyzed for S protein expression by SDS-PAGE and immunoblotting. Detection of vesicular stomatitis virus matrix protein (VSV-M) served as a loading control. (A and B, bottom) Immunoblots conducted for panels A ($n = 3$) and B ($n = 6$) were subjected to quantitative analysis using ImageJ software. S protein signals were normalized against the corresponding signals for ACTB or VSV-M, and expression and particle incorporation, respectively, of MERS-S WT were set as 100%. For S proteins that yielded two bands (S0 and S2), the two signals were combined before normalization. Mean values are shown; error bars indicate SEMs. Statistical significance of differences in particle expression or incorporation efficiency between MERS-S WT and variants was analyzed by paired two-tailed Student *t* tests.

D510G and I529T do not alter sialic acid dependency of viral entry. A recent study showed that MERS-S can bind to sialic acids, glycans presented on plasma membrane proteins and lipids, and that sialic acid engagement promotes S protein-driven entry (9). We enzymatically removed sialic acids by neuraminidase (NA) treatment to investigate whether the Korean polymorphisms or the polymorphisms found in the Middle East impact sialic acid dependence. Neuraminidase treatment markedly reduced influenza A virus hemagglutinin (HA)-driven entry but had no effect on entry driven by VSV-G (Fig. 4), as expected. Moreover, entry driven by MERS-S WT and S protein variants was comparably inhibited by neuraminidase treatment (Fig. 4), indicating that none of the amino acid changes in MERS-S altered sialic acid dependence of viral entry.

D510G and I529T do not alter the choice of MERS-S activating host cell protease. CatL and TMPRSS2 activate MERS-S in cell culture (10, 24), and the activity of TMPRSS2 or related enzymes is required for SARS-CoV spread in the host (26). Therefore, we investigated whether the polymorphisms under study modulated the capacity of MERS-S to employ CatL and TMPRSS2 for activation. For this, we first employed 293T cells, which express endogenous CatL but not TMPRSS2 and allow MERS-S-driven entry in a CatL-dependent fashion (10, 24). The cells were transfected with DPP4 plasmid and either TMPRSS2 encoding or empty plasmid (control), incubated with the CatL inhibitor MDL28170, and then analyzed for S protein-driven transduction. Incubation of control cells with MDL28170 reduced entry driven by MERS-S WT and S protein variants, and this effect was fully rescued by directed expression of TMPRSS2 (Fig. 5A). Next, we

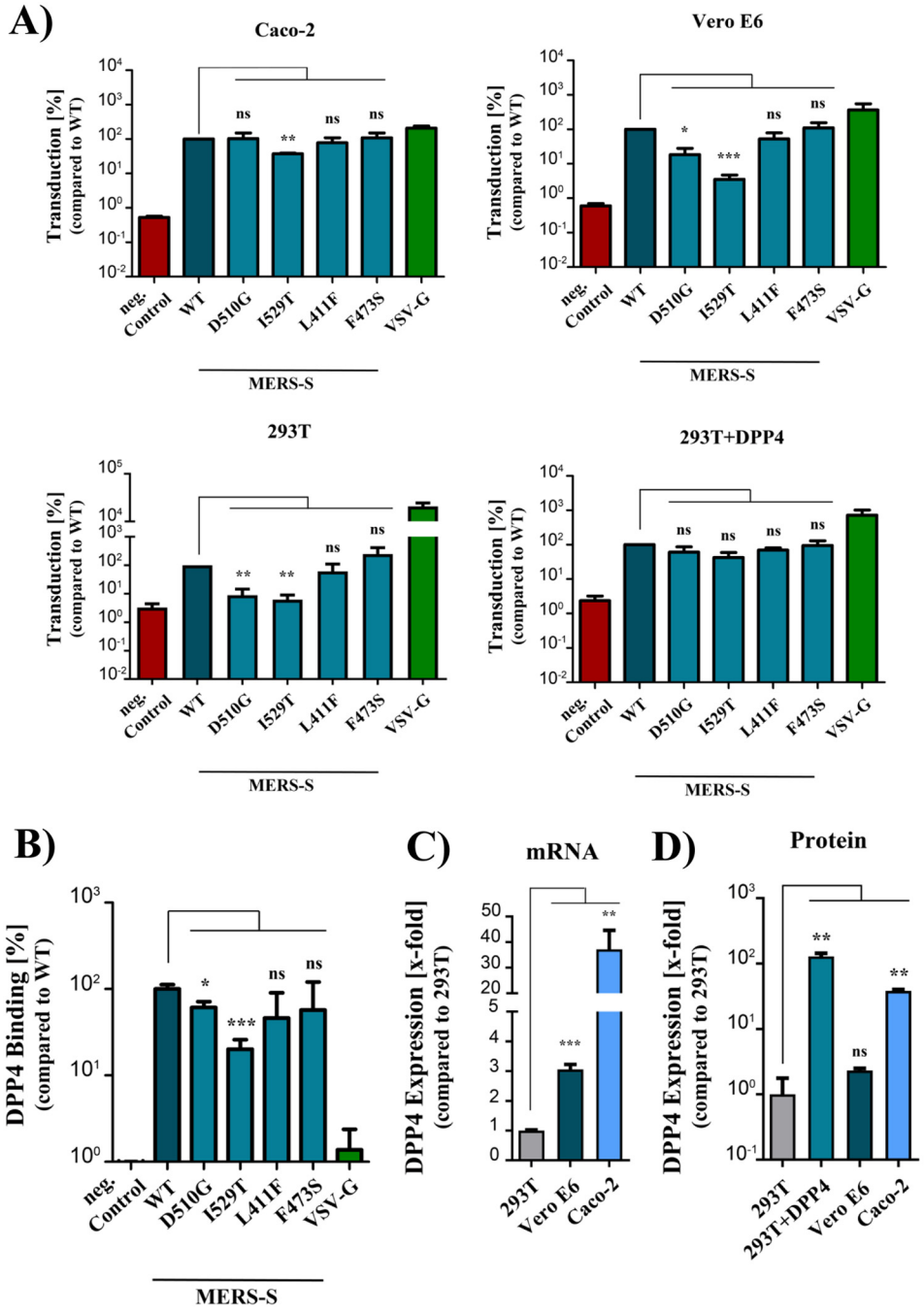

FIG 3 Polymorphisms found in the S proteins of Korean MERS patients allow robust entry into cells expressing large amounts of DPP4. (A) Equal volumes of rhabdoviral particles harboring MERS-S WT, the indicated S protein mutants, VSV-G (positive control), or no glycoprotein (negative control) were inoculated onto Caco-2, Vero E6, 293T, and 293T cells overexpressing DPP4. Transduction efficiency was quantified at 18 h posttransduction by measuring the activity of virus-encoded luciferase in cell lysates. Transduction mediated by MERS-S WT was set as 100%. The averages from three individual experiments performed with quadruplicate samples are shown; error bars indicate SEMs. (B) 293T cells transfected to express the indicated viral proteins or empty expression vector (control) were detached and incubated with human Fc-tagged, soluble DPP4 (solDPP4-Fc) and an Alexa Fluor 488-conjugated anti-human antibody before DPP4 binding was quantified by flow cytometry. For normalization, binding of solDPP4-Fc to MERS-S WT was set as 100%. The results of a single representative experiment carried out with triplicate samples are shown and were confirmed in a separate experiment. Error bars indicate SDs. (C) Total cellular RNA was extracted from the indicated cell lines, reverse transcribed to cDNA and DPP4 transcript levels were analyzed by quantitative PCR in combination with the $2^{-\Delta\Delta CT}$ method using ACTB as the housekeeping gene control and 293T cells as a reference (DPP4 level was set as 1). The results of a single representative experiment performed with triplicate samples are shown. Error bars indicate SDs. (D) Caco-2, Vero E6, and 293T cells (either untransfected or transfected with expression plasmid for DPP4) were analyzed for DPP4 cell surface expression by

(Continued on next page)

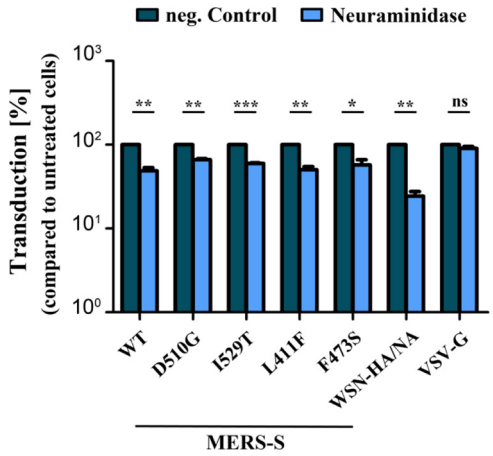

FIG 4 RBD polymorphisms do not modulate sialic acid dependence of MERS-S-driven host cell entry. Caco-2 cells were preincubated with recombinant neuraminidase or were left untreated (control) before being inoculated with rhabdoviral particles harboring MERS-S WT, the indicated S protein mutants, influenza A virus (WSN, subtype H1N1) hemagglutinin and neuraminidase (WSN-HA/NA), or VSV-G. At 18 h posttransduction, transduction efficiency was quantified by measuring the activity of virus-encoded luciferase in cell lysates. For normalization, transduction efficiency of untreated cells was set as 100%. The combined data from three independent experiments performed with quadruplicate samples are presented. Error bars indicate SEMs, and statistical significance was analyzed by paired two-tailed Student *t* tests.

investigated S protein activation in Caco-2 cells, which express endogenous TMPRSS2 (27) and afforded the opportunity to visualize a potentially more subtle impact of the S protein polymorphisms on activation by TMPRSS2. However, incubation of Caco-2 cells with rising concentrations of camostat mesylate, a TMPRSS2 inhibitor, comparably reduced entry driven by MERS-S WT and S protein variants and had no effect on VSV-G-mediated entry (Fig. 5B), as expected. These findings suggest that the polymorphisms under study did not compromise S protein activation by CatL and TMPRSS2 and did not endow the S protein with the ability to use low levels of TMPRSS2 activity with increased efficiency for S protein activation.

D510G and I529T do not modulate IFITM sensitivity. Expression of IFITM proteins is IFN inducible and inhibits MERS-S-driven entry into target cells (28), most likely at the stage of membrane fusion. We investigated whether the S protein polymorphisms under study modulated susceptibility of MERS-S-driven entry to blockade by IFITM proteins. For this, we employed 293T cells stably expressing IFITM1, IFITM2, and IFITM3. Expression of IFITM proteins had little effect on entry driven by the Machupo virus glycoprotein (MACV-GPC), while both IFITM2 and IFITM3 markedly reduced entry by the influenza A virus hemagglutinin (Fig. 6), in accordance with published data (28). Moreover, expression of IFITM2 but not IFITM1 and IFITM3 diminished MERS-S WT-mediated host cell entry, as expected, and similar effects were observed for the S protein variants analyzed (Fig. 6). Finally, comparable results were obtained with 293T cells transiently transfected with escalating amounts of IFTIM2 plasmid, although variant F473S showed a slightly reduced IFITM2 sensitivity under these conditions (data not shown). In sum, the RBD polymorphisms observed in Korean patients and MERS-CoV from the Middle East did not markedly alter IFITM sensitivity of viral entry.

D510G and I529T increase resistance to antibody-mediated neutralization. The antibody response significantly contributes to control of MERS-CoV infection in the host. Therefore, we asked whether the polymorphisms under study impact antibody-

FIG 3 Legend (Continued)
flow cytometry using anti-DPP4 and Alexa Fluor 488-conjugated anti-mouse antibodies. For normalization, DPP4 surface expression in untransfected 293T cells was set as 1. The results of a single, representative experiment performed with duplicate samples are shown; error bars indicate SDs. Similar results were obtained in two separate experiments. Statistical significance was analyzed by paired (A) or unpaired (B to D) two-tailed Student *t* tests.

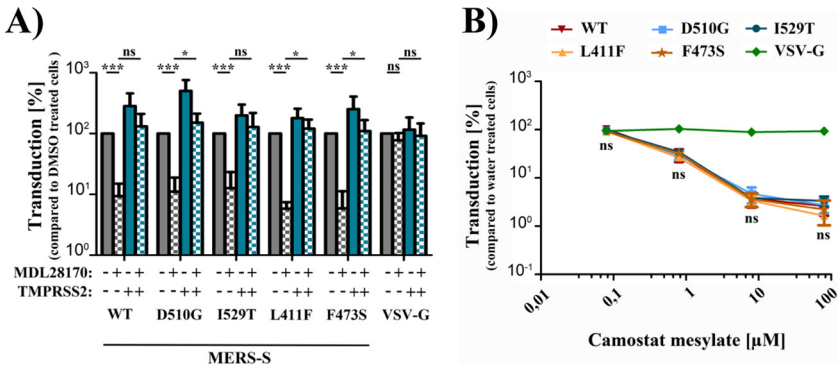

FIG 5 RBD polymorphisms do not impact MERS-S proteolytic activation. (A) 293T cells were transfected with expression plasmid for DPP4 alone (gray bars) or in combination with expression plasmid for TMPRSS2 (blue bars). At 24 h posttransfection, the cells were preincubated with dimethyl sulfoxide (DMSO; control [filled bars]) or cathepsin L inhibitor (MDL28170 [bars with checkerboard filling]) before being inoculated with rhabdoviral particles harboring MERS-S WT, the indicated S protein mutants, or VSV-G. Transduction efficiency was quantified by measuring the activity of virus-encoded luciferase in cell lysates at 18 h posttransduction. For normalization, luciferase activity measured for 293T cells overexpressing DPP4 and incubated with DMSO (filled gray bars) was set as 100%. (B) Caco-2 cells, for which MERS-S-driven entry relies on TMPRSS2 instead of cysteine proteases, were preincubated with medium containing water (control) or increasing concentrations of a TMPRSS2 inhibitor, camostat mesylate, before being inoculated with rhabdoviral pseudotypes harboring MERS-S WT, the indicated S protein mutants, or VSV-G. Transduction efficiency was quantified as described above. For normalization, transduction levels in the absence of inhibitor were set as 100%. The averages of four (A) or three (B) individual experiments performed with quadruplicate samples are shown. Error bars indicate SEMs. Statistical significance of differences of the indicated data pairs (A) or between WT and mutant S proteins (B) was analyzed by paired two-tailed Student *t* tests.

mediated neutralization. We focused our analysis on D510G and I529T since these changes modulated the efficiency of host cell entry. First, we tested whether D510G and I529T alter inhibition of S protein-driven entry by the murine antibody F11, which binds to an epitope encompassing amino acid 509, and macaque antibody JC57-14, which recognizes an epitope including amino acid 535 (29). Indeed, exchange D510G rendered MERS-S-driven entry insensitive to inhibition by F11, while I529T reduced

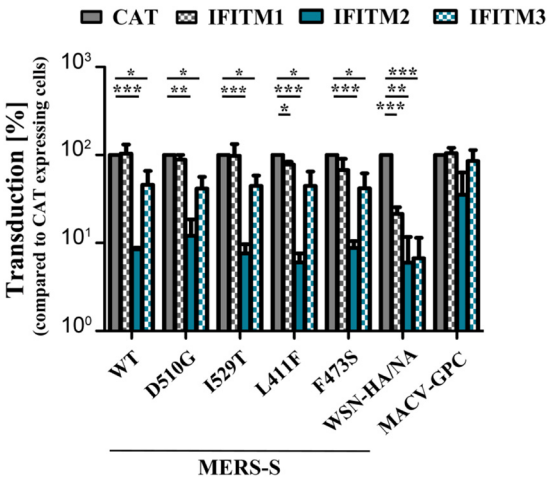

FIG 6 RBD polymorphisms do not change MERS-S sensitivity toward interferon-induced transmembrane proteins. 293T cells stably expressing interferon-induced transmembrane proteins (IFITM1 to -3) or chloramphenicol acetyltransferase (CAT; control) were transduced with rhabdoviral particles harboring MERS-S WT, the indicated S protein mutants, WSN-HA/NA, Machupo virus glycoprotein (MACV-GPC), or no viral glycoprotein (negative control; data not shown). At 18 h posttransduction, transduction efficiency was quantified by measuring the virus-encoded luciferase activity in cell lysates. For normalization, transduction of control 293T-CAT cells was set as 100%. The averages from three individual experiments performed with quadruplicate samples are shown. Error bars indicate SEMs, and statistical significance was analyzed by paired two-tailed Student *t* tests.

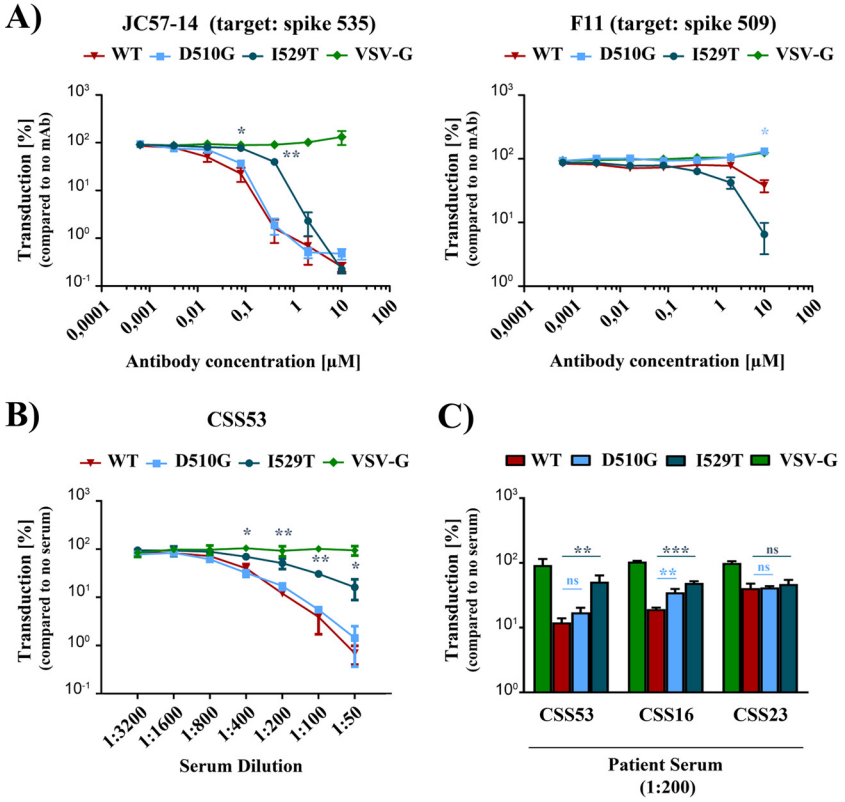

FIG 7 RBD polymorphisms increase resistance of MERS-S against antibody-mediated neutralization. Rhabdoviral particles harboring MERS-S WT, the indicated MERS-S mutants, or VSV-G were preincubated with increasing concentrations of MERS-S-specific monoclonal antibodies (mAb) that target different epitopes in the RBD (F11 or JC57-14) (A) or different dilutions of serum from a MERS patient (CSS53) (B) or a single dilution (1:200) of sera from three different MERS patients (CSS53 [data taken from panel B for direct comparison], CSS16, and CSS23) (C) before being inoculated onto Caco-2 cells. Cells transduced in the absence of mAb/serum served as controls. Transduction efficiency was quantified by measuring the activity of virus-encoded luciferase in cell lysates at 18 h posttransduction. For normalization, transduction in the absence of mAb/serum was set as 100%. The averages from three independent experiments performed with quadruplicate samples are presented in panel A; error bars indicate SEMs. Statistical significance of differences between transduction mediated by MERS-S WT and the S protein mutants was analyzed by paired two-tailed Student *t* tests. The results of a single representative experiment performed with triplicate samples are shown in panels B and C and were confirmed in a separate experiment. Error bars indicate SDs.

blockade of S protein-driven entry by JC57-14 (Fig. 7A). These findings encouraged us to investigate whether D510G and I529T alter susceptibility of MERS-S-driven host cell entry to inhibition by human sera obtained from MERS patients. For this, we studied sera of three patients who had acquired MERS-CoV infection in the Middle East and were admitted to German hospitals in Essen (serum CSS16), Osnabrück (CSS53), and Munich (CSS23) (Table 1). One serum sample was of sufficient quantity for detailed analysis (CSS53), while the others could be tested only at a single dilution (CSS16 and

TABLE 1 Information on the sera used in this study

Serum sample	Patient information[a]					Reference
	Age (yrs)	Origin[b]	Hospital[c]	Year	Disease outcome	
CSS16	45	Qatar	Essen	2012	Recovered	50
CSS23	73	UAE[d]	Munich	2013	Deceased	51
CSS53	65	UAE[d]	Osnabrück	2015	Deceased	52

[a]All patients were male.
[b]Country where the infection was acquired.
[c]German city where the patient was treated.
[d]UAE, United Arab Emirates.

CSS23). Remarkably, MERS-S harboring polymorphism D510G showed a significantly increased resistance against neutralization by one serum sample (CSS16), and polymorphism I529T diminished neutralization by two sera (CSS16 and CSS53 [Fig. 7B and C]). Finally, neither mutation had any impact on neutralization by serum sample CSS23. However, the overall neutralizing activity of this particular serum sample was reduced compared to those of the other sera tested and might have been too low to allow for differential neutralization of MERS-S WT and mutants D510G and I529T. In summary, our results suggest that increased resistance against humoral immune responses might have driven the emergence of the D510G and I529T variants.

DISCUSSION

The large MERS outbreak within hospitals in the Republic of Korea in 2015 raised the question of whether viral variants with increased transmissibility might have been responsible. Indeed, the majority of patients in Korea harbored viruses with at least one unique mutation in the RBD, D510G and/or I529T (13, 14). Unexpectedly, these mutations reduced DPP4 binding and viral entry (14), raising the question of whether they were beneficial to the virus. We found that D510G and I529T were compatible with robust S protein-driven entry into cells expressing large amounts of DPP4 and conferred resistance against antibody-mediated neutralization. These findings support the previously proposed concept that escape from antibody responses might shape MERS-CoV evolution and might come at the cost of reduced DPP4 binding (30). However, they also suggest that diminished DPP4 binding may not compromise the ability of MERS-CoV to spread in target cells expressing robust levels of DPP4.

The MERS outbreak in the Republic of Korea was initiated by a single infected traveler, comprised 186 cases and 38 deaths, and encompassed primary, secondary, tertiary, and quaternary infections (6, 7). The case-fatality rate was roughly 20% and was thus lower than that reported for MERS patients in the Middle East. This may have various reasons, including differences in patient care and virulence of the MERS-CoV strains responsible for the outbreaks (14). The I529T mutation has been detected in 72% of patients in Korea examined by one study and might have already been present in the index patient (14). Similarly, the S protein sequences from 26 out of 38 patients deposited in the virus variation database (https://www.ncbi.nlm.nih.gov/genome/viruses/variation/) contain the I529T change. Moreover, viruses harboring this mutation established secondary, tertiary, and quaternary infections (13, 14). In contrast, the D510G mutation was present in only 8% of patients analyzed in a previous study, and 6 out of 38 S protein sequences (16%) deposited in the virus variation database contained this exchange. Kim and colleagues reported that D510G and particularly I529T diminish binding of MERS-S to DPP4 and reduce entry into 293T cells transfected to express DPP4 (14). Moreover, structural evidence that these mutations disturb the interface between DPP4 and MERS-S was presented (14). However, it remained unclear whether these mutations may also aid virus spread under certain conditions.

Binding of MERS-S to DPP4 is essential for infectious host cell entry (8), and DPP4/S protein interactions are an important determinant of MERS-CoV species tropism (31). Moreover, patients with chronic lung disease were shown to express increased levels of DPP4 (32, 33) and are known to be at augmented risk of developing fatal MERS (34), suggesting that DPP4 levels expressed under physiologic conditions might limit viral spread in patients. Therefore, we investigated whether the previously reported negative effect of D510G and I529T on MERS-S-driven entry was dependent on DPP4 expression levels. Our results show that this is indeed the case: both mutations markedly reduced entry into 293T cells, which expressed low levels of endogenous DPP4 mRNA and protein, but had little effect on entry into Caco-2 cells, which express large amounts of DPP4. Robust expression of DPP4 has been detected in viral target cells in the human respiratory epithelium, type I and type II pneumocytes and alveolar macrophages (8, 32), and it is thus conceivable that WT virus and virus bearing D510G or I529T infect these cells with comparable efficiencies in the lung of MERS patients. Finally, one can speculate that engagement of attachment-promoting factors ex-

pressed in viral target cells in the human respiratory tract but not the cell lines studied here might allow mutants D510G and I529T to compensate for reduced DPP4 binding and to enter cells with the same efficiency as WT virus.

The proteolytic activation of MERS-S by host cell proteases is essential for MERS-S-driven entry into target cells (35). Therefore, we addressed whether D510G and I529T might augment viral spread by promoting S protein activation or by changing the choice of S protein-activating protease. Two interconnected routes have been described for MERS-S activation. Upon binding to DPP4, either the virus may be transported into host cell endosomes, where the S protein is activated by cathepsin L, or the S protein may be activated at the cell surface by TMPRSS2 (10, 11, 24). Notably, the choice between CatL and TMPRSS2 might be determined by S protein processing in the infected cell: S protein cleavage by furin in infected cells seems to be indispensable for subsequent DPP4-induced conformational changes in the S protein that are in turn essential for activation by TMPRSS2 (36). The present study demonstrates that D510G and I529T impact neither S protein cleavage by furin nor S protein activation by TMPRSS2 or CatL. This finding may not be unexpected since both residues are located distant to the two sites believed to be important for S protein processing and activation, R751 (S1/S2 site) and R887 (S2′ site).

Several cellular factors can modulate the efficiency of MERS-S-driven entry into cells, raising the question of whether D510G and I529T might alter their effects in a way that promotes viral spread. The DPP4 ligand adenosine deaminase, which is highly expressed in lymphoid tissue and constitutes a component of the purine salvage pathway (37), has been shown to compete with MERS-S for DPP4 binding and to block MERS-S-driven entry into target cells (31). Moreover, the IFN-induced transmembrane proteins IFITM2 and, to a lesser degree, IFITM3 were demonstrated to block MERS-S-driven entry, at least upon overexpression (28). Finally, MERS-S has been shown to bind to a coreceptor, sialic acid, which promotes viral entry into target cells (9). Our results indicate that D510G and I529T do not impact the above-named processes, suggesting that both mutations might affect neither viral attachment to cells nor the membrane fusion reaction.

The spike protein is the key target of neutralizing antibodies, and such antibodies are detected with high frequency in convalescent MERS patients who have survived severe disease (18, 38–40). Neutralizing antibodies can be directed against the RBD and interfere with viral entry by blocking DPP4/S protein interactions. A previous study conducted with cell culture systems found that MERS-CoV can acquire mutations that allow escape from RBD-targeting neutralizing antibodies but also provided evidence that such mutations might come at the cost of decreased DPP4 binding and viral fitness (30). Such a scenario generally matches our findings that D510G and I529T render the S protein at least partially resistant against neutralization by monoclonal antibodies and sera from MERS patients and reduce DPP4 binding. However, our results also allow the speculation that reduced DPP4 binding might not necessarily translate into reduced viral spread in host cells expressing high levels of DPP4. This possibility awaits confirmation with infectious MERS-CoV and primary target cells. Nevertheless, it would be in keeping with the observation that viruses harboring the I529T change were robustly transmitted between patients during the MERS outbreak in the Republic of Korea (14), although the I529T change did not provide the virus with an advantage in the absence of humoral responses. Finally, our finding that single point mutations in MERS-S can increase resistance to antibody-mediated neutralization highlights the need to develop vaccines and therapeutics that simultaneously target multiple epitopes in MERS-S.

Collectively, our findings and previous work suggest that MERS-CoV variants with at least partial resistance to antibody-mediated neutralization can retain high infectivity for cells expressing robust amounts of DPP4 and can spread between humans.

MATERIALS AND METHODS

Plasmids. We employed expression plasmids encoding the VSV glycoprotein (VSV-G) (41), Machupo virus glycoprotein (MACV-GPC) (42) (kindly provided by M. Farzan), influenza A virus strain A/WSN/33

(H1N1) hemagglutinin and neuraminidase (WSN-HA/NA) (43), and WT MERS-S (10), which have been described elsewhere. In addition, we employed overlap extension PCR to generate MERS-S mutants harboring single (L411F, F473S, D510G, and I529T) mutations in the RBD (primer sequences and detailed information on the cloning procedure are available upon request). For all S proteins, we also generated versions containing a C-terminal V5 epitope for detection by immunoblotting. Expression plasmids for TMPRSS2 N-terminally fused to a cMYC epitope and DPP4 N-terminally fused to DsRed (EU827527.1 and DsRed-DPP4) were constructed by amplifying the genetic information from existing expression plasmids and cloning the respective open reading frame (ORF) into the pQCXIP plasmid (kindly provided by A. L. Brass). For the TMPRSS2 expression vector, we further exchanged the selection marker for puromycin resistance by that for blasticidin resistance, which was taken from plasmid pcDNA6/TR vector (8, 44). All PCR-amplified sequences were subjected to automated sequence analysis (Microsynth SeqLab) to verify their integrity.

Cell culture. 293T (human) and Vero E6 (African green monkey) cells were cultivated in Dulbecco's modified Eagle's medium (DMEM; PAN-Biotech). In addition, the human colorectal adenocarcinoma cell line Caco-2 was grown in minimum essential medium (MEM; Thermo Fisher Scientific). 293T cells stably expressing IFITMs or chloramphenicol acetyltransferase (CAT), 293T-IFITM1, 293T-IFITM2, 293T-IFITM3, and 293T-CAT (45), were cultivated as for the parental 293T cell line with the exception that they additionally received 0.5 μg/ml of puromycin (Biomol). All media were supplemented with 10% fetal bovine serum (FBS; PAN-Biotech) as well as 1× penicillin and streptomycin from a 100× stock solution (PAN-Biotech). All cell lines were cultivated in a humidified atmosphere at 37°C and 5% CO_2. Transfection of 293T cells was performed by calcium phosphate precipitation.

Protease inhibitors. We employed inhibitors targeting cathepsin L and related proteases (MDL28170; Sigma-Aldrich) or TMPRSS2 and related proteases (camostat mesylate; Sigma-Aldrich). Target cells for transduction experiments were treated with the respective inhibitor (specific concentrations are indicated in the legends of the respective figures) for 2 h prior to inoculation with rhabdoviral transduction vectors.

Neuraminidase treatment of target cells. To remove terminal sialic acids from macromolecules on the cell surface, target cells were preincubated with 100 mU of recombinant neuraminidase (Sigma-Aldrich) for 2 h before being inoculated with rhabdoviral transduction vectors.

Production of rhabdoviral transduction vectors and transduction of target cells. We employed rhabdoviral transduction vectors (pseudoparticles/pseudotypes) based on a replication-deficient vesicular stomatitis virus that lacks the genetic information for VSV-G but contains ORFs for enhanced green fluorescent protein (eGFP) and firefly luciferase (fLuc), VSV*ΔG-fLuc (46). For production of VSV-based pseudotypes (VSVpp), 293T cells were transfected with expression plasmids for MERS-S WT, mutant MERS-S harboring RBD polymorphisms, MACV-GPC, H1N1(WSN)-HA/NA, VSV-G (positive control) or empty expression vector (negative control). At 24 h posttransfection, cells were inoculated with VSV-G-transcomplemented VSV*ΔG-fLuc (Indiana strain, kindly provided by G. Zimmer) at a multiplicity of infection of 3 and incubated for 1 h at 37°C and 5% CO_2. Next the inoculum was removed, cells were washed with phosphate-buffered saline (PBS), and standard culture medium which contained anti-VSV-G antibody (I1, mouse hybridoma supernatant from CRL-2700; ATCC) was added to neutralize residual input virus (cells transfected with VSV-G expression plasmid received culture medium without anti-VSV-G antibody). The cells were further incubated for 24 h before the supernatant was harvested, freed from cellular debris by centrifugation (3,000 × *g* for 10 min), and either stored at −80°C or used for transduction experiments. For the latter, target cells were grown in 96-well plates. If necessary, target cells were previously transfected with expression plasmids for DsRed-DPP4 and/or TMPRSS2 (24 h in advance) or were pretreated with protease inhibitors or neuraminidase (2 h in advance). For transduction, the culture medium was aspirated and the rhabdoviral transduction vectors were added to the cells. Transduction efficiency was quantified by measuring the virus-encoded fLuc activity in cell lysates using commercial kits (Beetle Juice; PJK) and a plate luminometer (Hidex, Turku, Finland) as described elsewhere (47).

Analysis of MERS-S expression and incorporation into VSVpp. 293T cells were transfected with expression plasmids for C-terminally V5-tagged versions of the MERS-S WT or MERS-S mutants or were control transfected with empty plasmid (negative control). At 48 h posttransfection, the culture supernatant was removed, cells were washed with PBS, and whole cells lysates (WCL) were prepared as follows. First, 2×SDS sample buffer (0.03 M Tris-HCl, 10% glycerol, 2% SDS, 5% beta-mercaptoethanol, 0.2% bromophenol blue, 1 mM EDTA) was added to the cells, which were then incubated for 10 min before the sample was transferred to 1.5-ml reaction tubes and heated to 95°C for additional 10 min. For analysis of S protein incorporation into VSV particles, the respective culture supernatants were pelleted by high-speed centrifugation (25,000 × *g*, 120 min, and 4°C) through a 20% (wt/vol) sucrose cushion, mixed with 2× SDS sample buffer, and heated to 95°C for additional 10 min. Following SDS-PAGE, proteins were transferred onto nitrocellulose membranes (Hartenstein GmbH) by immunoblotting. The membranes were then blocked by incubation in 5% skim milk in PBS–0.5% Tween 20 (PBS-T) for 30 min at room temperature (RT) and then incubated with primary antibody solution (anti-V5, anti-ACTB, or anti-VSV-M) overnight at 4°C. Next membranes were washed with PBS-T and further incubated with secondary antibody solution (anti-mouse-horseradish peroxidase [HRP]) for 1 h at RT. After additional washing steps, the membranes were finally developed using an in house-made chemiluminescence reagent in combination with the ChemoCam imaging system and ChemoStar Professional software (Intas Science Imaging Instruments GmbH). For quantification of the signal intensity, the program ImageJ (FIJI distribution) (48) was used. S protein signals detected in the WCL and supernatants were normalized against the respective signals of the loading control, either ACTB or VSV-M.

Antibodies for protein detection in immunoblot analysis. The following antibodies were used as primary antibodies: anti-V5 (mouse, 1:1,000; Thermo Fisher Scientific), anti-β-actin (ACTB, mouse, 1:1,000; Sigma-Aldrich), and anti-VSV-M (mouse, 1:1,000; Kerafast). As a secondary antibody, an HRP-coupled anti-mouse antibody was used (goat, 1:5,000; Dianova). All antibodies were diluted in PBS-T (Carl Roth) and 5% skim milk (Carl Roth).

Analysis of MERS-S/DPP4 interaction and DPP4 surface expression by flow cytometry. For the detection of MERS-S/DPP4 interaction, 293T cells were transfected with expression plasmids for MERS-S WT, MERS-S mutants, or VSV-G or empty plasmid (both negative controls). At 48 h posttransfection, the cells were washed with PBS and then resuspended in 1% bovine serum albumin (BSA)-PBS. Next, the cells were pelleted by centrifugation (5 min at 600 $\times$ *g* at 4°C) and resuspended in 1% BSA-PBS containing soluble DPP4 equipped with a C-terminal human Fc tag (solDPP4-Fc, 1:200; ACROBiosystems). After incubation for 1 h at 4°C, the cells were washed with 1% BSA-PBS and then resuspended in 1% BSA-PBS containing an Alexa Fluor 488-conjugated anti-human antibody (1:500; Thermo Fisher Scientific). After another incubation period (as described above), cells were washed with 1% BSA-PBS, fixed with 4% paraformaldehyde solution, and analyzed by flow cytometry as described below. For the analysis of DPP4 surface expression by flow cytometry, 293T (untransfected or transfected with expression plasmid for DPP4), Caco-2, and Vero E6 cells were detached by resuspension in 1% BSA-PBS (293T cells) or by incubation in citric saline (PBS containing 0.135 M potassium chloride and 0.015 M sodium citrate; Caco-2 and Vero E6 cells). Cells were then pelleted and washed as described above, successively incubated with anti-DPP4 (mouse, 1:200; Abcam) and Alexa Fluor 488-conjugated anti-mouse (goat, 1:500; Thermo Fisher Scientific) antibodies, and fixed. Finally, all samples were analyzed using an LSR II flow cytometer and the FACS Diva software (both from BD Biosciences). For further data analysis, FCS Express 4 Flow research software (De Novo software) was employed.

Quantification of DPP4-specific transcript levels by qPCR. Total cellular RNA was extracted from 293T, Caco-2, and Vero E6 cells using the RNeasy minikit (Qiagen) according to the manufacturer's instructions. Then 1 μg of RNA was treated with DNase (New England BioLabs) and reverse transcribed into cDNA using the SuperScript III first-strand synthesis system (Thermo Fisher Scientific), both following the manufacturers' specifications. Subsequently, 1 μl of each sample was subjected to quantitative PCR (qPCR) using the QuantiTect SYBR green PCR kit (Qiagen) and a Rotor-Gene Q platform (Qiagen). All samples were analyzed for β-actin (housekeeping gene control) and DPP4 (gene of interest) transcripts in triplicates. Finally, data were analyzed based on the threshold cycle ($2^{-\Delta\Delta CT}$) method (49) using 293T cells as a reference.

Neutralization experiments. Rhabdoviral transduction vectors harboring MERS-S WT, MERS-S mutants, or VSV-G were normalized for comparable transduction of Caco-2 cells ($\sim 10^5$ luminescent counts/s), incubated for 30 min at RT with increasing concentrations of monoclonal antibodies targeting distinct epitopes within the MERS-S RBD, JC57-14 (targeting an epitope around amino acid residue 535 in MERS-S, isolated from vaccinated nonhuman primates [PDB code 6C6Y]) and F11 (targeting an epitope around amino acid residue 509 in MERS-S, isolated from vaccinated mice) (29) or with different dilutions of serum from a MERS patient who traveled from the Arabian Peninsula to Germany. Furthermore, sera from two additional MERS patients, CSS16 and CSS23, were tested at a dilution of 1:200 (since the amount of those sera was limited, they were tested at a fixed dilution). Please see Table 1 for further information on the sera and the patient histories. Afterwards, the mixtures of VSVpp and antibodies/serum were inoculated onto Caco-2 cells that were further incubated at 37°C and 5% CO_2. At 18 h posttransduction, transduction efficiency was quantified (as described above). For normalization, transduction efficiency of rhabdoviral transduction vectors that were incubated in the absence of antibodies/serum was set as 100%.

Statistical analysis. If not stated otherwise, unpaired or paired, two-tailed Student *t* tests were performed to test statistical significance of data originating from single representative or multiple combined experiments, respectively. In figures, statistical significance is represented as follows: *, $P \leq 0.05$; **, $P \leq 0.01$; ***, $P \leq 0.001$; and ns, not significant.

ACKNOWLEDGMENTS

We are grateful to M. Farzan, A. L. Brass, and G. Zimmer for providing expression plasmids and reagents.

This work was supported, including the efforts of Stefan Pöhlmann and Christian Drosten, by the Bundesministerium für Bildung und Forschung within the network project RAPID (Risikobewertung bei präpandemischen respiratorischen Infektionserkrankungen; 01KI1723D and 01KI1723A). Furthermore, this work was supported by intramural funding to Barney S. Graham through the National Institutes of Health (NIH).

The funders had no role in study design, data collection and interpretation, or the decision to submit the work for publication.

Charité-Universitätsmedizin Berlin is a corporate member of Freie Universität Berlin, Humboldt-Universität zu Berlin, and Berlin Institute of Health. The German Centre for Infection Research is an associated partner of Charité-Universitätsmedizin Berlin.

REFERENCES

1. Lai MMC, Perlman S, Anderson LJ. 2007. Coronaviridae, p 1305–1336. *In* Knipe DM, Howley PM, Griffin DE, Lamb RA, Martin MA, Roizman B, Straus SE (ed), Fields virology, 5th ed, vol 1. Lippincott, Williams & Wilkins, Philadelphia, PA.
2. Haagmans BL, Al Dhahiry SH, Reusken CB, Raj VS, Galiano M, Myers R, Godeke GJ, Jonges M, Farag E, Diab A, Ghobashy H, Alhajri F, Al-Thani M, Al-Marri SA, Al Romaihi HE, Al Khal A, Bermingham A, Osterhaus AD, AlHajri MM, Koopmans MP. 2014. Middle East respiratory syndrome coronavirus in dromedary camels: an outbreak investigation. Lancet Infect Dis 14:140–145. https://doi.org/10.1016/S1473-3099(13)70690-X.
3. Reusken CBEM, Haagmans BL, Müller MA, Gutierrez C, Godeke G-J, Meyer B, Muth D, Raj VS, Smits-De Vries L, Corman VM, Drexler J-F, Smits SL, El Tahir YE, De Sousa R, van Beek J, Nowotny N, van Maanen K, Hidalgo-Hermoso E, Bosch B-J, Rottier P, Osterhaus A, Gortázar-Schmidt C, Drosten C, Koopmans MPG. 2013. Middle East respiratory syndrome coronavirus neutralising serum antibodies in dromedary camels: a comparative serological study. Lancet Infect Dis 13:859–866. https://doi.org/10.1016/S1473-3099(13)70164-6.
4. World Health Organization. 2018. Middle East respiratory syndrome coronavirus (MERS-CoV)—Saudi Arabia. http://www.emro.who.int/pandemic-epidemic-diseases/mers-cov/mers-situation-update-march-2018.html. Accessed 27 July 2018.
5. Assiri A, McGeer A, Perl TM, Price CS, Al Rabeeah AA, Cummings DA, Alabdullatif ZN, Assad M, Almulhim A, Makhdoom H, Madani H, Alhakeem R, Al-Tawfiq JA, Cotten M, Watson SJ, Kellam P, Zumla AI, Memish ZA, KSA MERS-CoV Investigation Team. 2013. Hospital outbreak of Middle East respiratory syndrome coronavirus. N Engl J Med 369:407–416. https://doi.org/10.1056/NEJMoa1306742.
6. Cho SY, Kang JM, Ha YE, Park GE, Lee JY, Ko JH, Lee JY, Kim JM, Kang CI, Jo IJ, Ryu JG, Choi JR, Kim S, Huh HJ, Ki CS, Kang ES, Peck KR, Dhong HJ, Song JH, Chung DR, Kim YJ. 2016. MERS-CoV outbreak following a single patient exposure in an emergency room in South Korea: an epidemiological outbreak study. Lancet 388:994–1001. https://doi.org/10.1016/S0140-6736(16)30623-7.
7. Oh MD, Park WB, Park SW, Choe PG, Bang JH, Song KH, Kim ES, Kim HB, Kim NJ. 2018. Middle East respiratory syndrome: what we learned from the 2015 outbreak in the Republic of Korea. Korean J Intern Med 33:233–246. https://doi.org/10.3904/kjim.2018.031.
8. Raj VS, Mou H, Smits SL, Dekkers DH, Muller MA, Dijkman R, Muth D, Demmers JA, Zaki A, Fouchier RA, Thiel V, Drosten C, Rottier PJ, Osterhaus AD, Bosch BJ, Haagmans BL. 2013. Dipeptidyl peptidase 4 is a functional receptor for the emerging human coronavirus-EMC. Nature 495:251–254. https://doi.org/10.1038/nature12005.
9. Li W, Hulswit RJG, Widjaja I, Raj VS, McBride R, Peng W, Widagdo W, Tortorici MA, van Dieren B, Lang Y, van Lent JWM, Paulson JC, de Haan CAM, de Groot RJ, van Kuppeveld FJM, Haagmans BL, Bosch BJ. 2017. Identification of sialic acid-binding function for the Middle East respiratory syndrome coronavirus spike glycoprotein. Proc Natl Acad Sci U S A 114:E8508–E8517. https://doi.org/10.1073/pnas.1712592114.
10. Gierer S, Bertram S, Kaup F, Wrensch F, Heurich A, Krämer-Kühl A, Welsch K, Winkler M, Meyer B, Drosten C, Dittmer U, von Hahn T, Simmons G, Hofmann H, Pöhlmann S. 2013. The spike protein of the emerging betacoronavirus EMC uses a novel coronavirus receptor for entry, can be activated by TMPRSS2, and is targeted by neutralizing antibodies. J Virol 87:5502–5511. https://doi.org/10.1128/JVI.00128-13.
11. Qian Z, Dominguez SR, Holmes KV. 2013. Role of the spike glycoprotein of human Middle East respiratory syndrome coronavirus (MERS-CoV) in virus entry and syncytia formation. PLoS One 8:e76469. https://doi.org/10.1371/journal.pone.0076469.
12. Shirato K, Kanou K, Kawase M, Matsuyama S. 2017. Clinical isolates of human coronavirus 229E bypass the endosome for cell entry. J Virol 91:e01387-16. https://doi.org/10.1128/JVI.01387-16.
13. Kim DW, Kim YJ, Park SH, Yun MR, Yang JS, Kang HJ, Han YW, Lee HS, Kim HM, Kim H, Kim AR, Heo DR, Kim SJ, Jeon JH, Park D, Kim JA, Cheong HM, Nam JG, Kim K, Kim SS. 2016. Variations in spike glycoprotein gene of MERS-CoV, South Korea, 2015. Emerg Infect Dis 22:100–104. https://doi.org/10.3201/eid2201.151055.
14. Kim Y, Cheon S, Min CK, Sohn KM, Kang YJ, Cha YJ, Kang JI, Han SK, Ha NY, Kim G, Aigerim A, Shin HM, Choi MS, Kim S, Cho HS, Kim YS, Cho NH. 2016. Spread of mutant Middle East respiratory syndrome coronavirus with reduced affinity to human CD26 during the South Korean outbreak. mBio 7:e00019-16. https://doi.org/10.1128/mBio.00019-16.
15. Drosten C, Muth D, Corman VM, Hussain R, Al Masri M, HajOmar W, Landt O, Assiri A, Eckerle I, Al Shangiti A, Al-Tawfiq JA, Albarrak A, Zumla A, Rambaut A, Memish ZA. 2015. An observational, laboratory-based study of outbreaks of Middle East respiratory syndrome coronavirus in Jeddah and Riyadh, Kingdom of Saudi Arabia, 2014. Clin Infect Dis 60:369–377. https://doi.org/10.1093/cid/ciu812.
16. Fagbo SF, Skakni L, Chu DK, Garbati MA, Joseph M, Peiris M, Hakawi AM. 2015. Molecular epidemiology of hospital outbreak of Middle East respiratory syndrome, Riyadh, Saudi Arabia, 2014. Emerg Infect Dis 21:1981–1988. https://doi.org/10.3201/eid2111.150944.
17. Sabir JS, Lam TT, Ahmed MM, Li L, Shen Y, Abo-Aba SE, Qureshi MI, Abu-Zeid M, Zhang Y, Khiyami MA, Alharbi NS, Hajrah NH, Sabir MJ, Mutwakil MH, Kabli SA, Alsulaimany FA, Obaid AY, Zhou B, Smith DK, Holmes EC, Zhu H, Guan Y. 2016. Co-circulation of three camel coronavirus species and recombination of MERS-CoVs in Saudi Arabia. Science 351:81–84. https://doi.org/10.1126/science.aac8608.
18. Corman VM, Albarrak AM, Omrani AS, Albarrak MM, Farah ME, Almasri M, Muth D, Sieberg A, Meyer B, Assiri AM, Binger T, Steinhagen K, Lattwein E, Al-Tawfiq J, Muller MA, Drosten C, Memish ZA. 2016. Viral shedding and antibody response in 37 patients with Middle East respiratory syndrome coronavirus infection. Clin Infect Dis 62:477–483. https://doi.org/10.1093/cid/civ951.
19. Hemida MG, Alnaeem A, Chu DK, Perera RA, Chan SM, Almathen F, Yau E, Ng BC, Webby RJ, Poon LL, Peiris M. 2017. Longitudinal study of Middle East respiratory syndrome coronavirus infection in dromedary camel herds in Saudi Arabia, 2014-2015. Emerg Microbes Infect 6:e56. https://doi.org/10.1038/emi.2017.44.
20. Hoffmann M, González Hernández M, Berger E, Marzi A, Pöhlmann S. 2016. The glycoproteins of all filovirus species use the same host factors for entry into bat and human cells but entry efficiency is species dependent. PLoS One 11:e0149651. https://doi.org/10.1371/journal.pone.0149651.
21. Fukuma A, Tani H, Taniguchi S, Shimojima M, Saijo M, Fukushi S. 2015. Inability of rat DPP4 to allow MERS-CoV infection revealed by using a VSV pseudotype bearing truncated MERS-CoV spike protein. Arch Virol 160:2293–2300. https://doi.org/10.1007/s00705-015-2506-z.
22. Gierer S, Muller MA, Heurich A, Ritz D, Springstein BL, Karsten CB, Schendzielorz A, Gnirss K, Drosten C, Pohlmann S. 2015. Inhibition of proprotein convertases abrogates processing of the Middle Eastern respiratory syndrome coronavirus spike protein in infected cells but does not reduce viral infectivity. J Infect Dis 211:889–897. https://doi.org/10.1093/infdis/jiu407.
23. Millet JK, Whittaker GR. 2014. Host cell entry of Middle East respiratory syndrome coronavirus after two-step, furin-mediated activation of the spike protein. Proc Natl Acad Sci U S A 111:15214–15219. https://doi.org/10.1073/pnas.1407087111.
24. Shirato K, Kawase M, Matsuyama S. 2013. Middle East respiratory syndrome coronavirus infection mediated by the transmembrane serine protease TMPRSS2. J Virol 87:12552–12561. https://doi.org/10.1128/JVI.01890-13.
25. Yang Y, Liu C, Du L, Jiang S, Shi Z, Baric RS, Li F. 2015. Two mutations were critical for bat-to-human transmission of Middle East respiratory syndrome coronavirus. J Virol 89:9119–9123. https://doi.org/10.1128/JVI.01279-15.
26. Zhou Y, Vedantham P, Lu K, Agudelo J, Carrion R, Jr, Nunneley JW, Barnard D, Pohlmann S, McKerrow JH, Renslo AR, Simmons G. 2015. Protease inhibitors targeting coronavirus and filovirus entry. Antiviral Res 116:76–84. https://doi.org/10.1016/j.antiviral.2015.01.011.
27. Bertram S, Dijkman R, Habjan M, Heurich A, Gierer S, Glowacka I, Welsch K, Winkler M, Schneider H, Hofmann-Winkler H, Thiel V, Pöhlmann S. 2013. TMPRSS2 activates the human coronavirus 229E for cathepsin-independent host cell entry and is expressed in viral target cells in the respiratory epithelium. J Virol 87:6150–6160. https://doi.org/10.1128/JVI.03372-12.
28. Wrensch F, Winkler M, Pohlmann S. 2014. IFITM proteins inhibit entry driven by the MERS-coronavirus spike protein: evidence for cholesterol-independent mechanisms. Viruses 6:3683–3698. https://doi.org/10.3390/v6093683.
29. Wang L, Shi W, Chappell JD, Joyce MG, Zhang Y, Kanekiyo M, Becker MM, van Doremalen N, Fischer R, Wang N, Corbett KS, Choe M, Mason RD, Van

Galen JG, Zhou T, Saunders KO, Tatti KM, Haynes LM, Kwong PD, Modjarrad K, Kong WP, McLellan JS, Denison MR, Munster VJ, Mascola JR, Graham BS. 2018. Importance of neutralizing monoclonal antibodies targeting multiple antigenic sites on MERS-CoV spike to avoid neutralization escape. J Virol 92:e02002-17. https://doi.org/10.1128/JVI.02002-17.

30. Tang XC, Agnihothram SS, Jiao Y, Stanhope J, Graham RL, Peterson EC, Avnir Y, Tallarico AS, Sheehan J, Zhu Q, Baric RS, Marasco WA. 2014. Identification of human neutralizing antibodies against MERS-CoV and their role in virus adaptive evolution. Proc Natl Acad Sci U S A 111:E2018–E2026. https://doi.org/10.1073/pnas.1402074111.
31. Raj VS, Smits SL, Provacia LB, van den Brand JM, Wiersma L, Ouwendijk WJ, Bestebroer TM, Spronken MI, van Amerongen G, Rottier PJ, Fouchier RA, Bosch BJ, Osterhaus AD, Haagmans BL. 2014. Adenosine deaminase acts as a natural antagonist for dipeptidyl peptidase 4-mediated entry of the Middle East respiratory syndrome coronavirus. J Virol 88:1834–1838. https://doi.org/10.1128/JVI.02935-13.
32. Meyerholz DK, Lambertz AM, McCray PB, Jr. 2016. Dipeptidyl peptidase 4 distribution in the human respiratory tract: implications for the Middle East respiratory syndrome. Am J Pathol 186:78–86. https://doi.org/10.1016/j.ajpath.2015.09.014.
33. Seys LJM, Widagdo W, Verhamme FM, Kleinjan A, Janssens W, Joos GF, Bracke KR, Haagmans BL, Brusselle GG. 2018. DPP4, the Middle East respiratory syndrome coronavirus receptor, is upregulated in lungs of smokers and chronic obstructive pulmonary disease patients. Clin Infect Dis 66:45–53. https://doi.org/10.1093/cid/cix741.
34. Zumla A, Hui DS, Perlman S. 2015. Middle East respiratory syndrome. Lancet 386:995–1007. https://doi.org/10.1016/S0140-6736(15)60454-8.
35. Hoffmann M, Hofmann-Winkler H, Pohlmann S. 2018. Priming time: how cellular proteases arm coronavirus spike proteins, p 71–98. *In* Böttcher-Friebertshäuser E, Garten W, Klenk HD (ed), Activation of viruses by host proteases. Springer International Publishing, Cham, Switzerland.
36. Park JE, Li K, Barlan A, Fehr AR, Perlman S, McCray PB, Jr, Gallagher T. 2016. Proteolytic processing of Middle East respiratory syndrome coronavirus spikes expands virus tropism. Proc Natl Acad Sci U S A 113:12262–12267. https://doi.org/10.1073/pnas.1608147113.
37. Cortes A, Gracia E, Moreno E, Mallol J, Lluis C, Canela EI, Casado V. 2015. Moonlighting adenosine deaminase: a target protein for drug development. Med Res Rev 35:85–125. https://doi.org/10.1002/med.21324.
38. Choe PG, Perera R, Park WB, Song KH, Bang JH, Kim ES, Kim HB, Ko LWR, Park SW, Kim NJ, Lau EHY, Poon LLM, Peiris M, Oh MD. 2017. MERS-CoV antibody responses 1 year after symptom onset, South Korea, 2015. Emerg Infect Dis 23:1079–1084. https://doi.org/10.3201/eid2307.170310.
39. Arabi YM, Hajeer AH, Luke T, Raviprakash K, Balkhy H, Johani S, Al-Dawood A, Al-Qahtani S, Al-Omari A, Al-Hameed F, Hayden FG, Fowler R, Bouchama A, Shindo N, Al-Khairy K, Carson G, Taha Y, Sadat M, Alahmadi M. 2016. Feasibility of using convalescent plasma immunotherapy for MERS-CoV infection, Saudi Arabia. Emerg Infect Dis 22:1554–1561. https://doi.org/10.3201/eid2209.151164.
40. Zhao J, Alshukairi AN, Baharoon SA, Ahmed WA, Bokhari AA, Nehdi AM, Layqah LA, Alghamdi MG, Al Gethamy MM, Dada AM, Khalid I, Boujelal M, Al Johani SM, Vogel L, Subbarao K, Mangalam A, Wu C, Ten Eyck P, Perlman S, Zhao J. 2017. Recovery from the Middle East respiratory syndrome is associated with antibody and T-cell responses. Sci Immunol 2:eaan5393. https://doi.org/10.1126/sciimmunol.aan5393.
41. Brinkmann C, Hoffmann M, Lübke A, Nehlmeier I, Krämer-Kühl A, Winkler M, Pöhlmann S. 2017. The glycoprotein of vesicular stomatitis virus promotes release of virus-like particles from tetherin-positive cells. PLoS One 12:e0189073. https://doi.org/10.1371/journal.pone.0189073.
42. Radoshitzky SR, Abraham J, Spiropoulou CF, Kuhn JH, Nguyen D, Li W, Nagel J, Schmidt PJ, Nunberg JH, Andrews NC, Farzan M, Choe H. 2007. Transferrin receptor 1 is a cellular receptor for New World haemorrhagic fever arenaviruses. Nature 446:92–96. https://doi.org/10.1038/nature05539.
43. Chaipan C, Kobasa D, Bertram S, Glowacka I, Steffen I, Tsegaye TS, Takeda M, Bugge TH, Kim S, Park Y, Marzi A, Pohlmann S. 2009. Proteolytic activation of the 1918 influenza virus hemagglutinin. J Virol 83:3200–3211. https://doi.org/10.1128/JVI.02205-08.
44. Bertram S, Glowacka I, Blazejewska P, Soilleux E, Allen P, Danisch S, Steffen I, Choi SY, Park Y, Schneider H, Schughart K, Pohlmann S. 2010. TMPRSS2 and TMPRSS4 facilitate trypsin-independent spread of influenza virus in Caco-2 cells. J Virol 84:10016–10025. https://doi.org/10.1128/JVI.00239-10.
45. Wrensch F, Hoffmann M, Gartner S, Nehlmeier I, Winkler M, Pohlmann S. 2017. Virion background and efficiency of virion incorporation determine susceptibility of simian immunodeficiency virus env-driven viral entry to inhibition by IFITM proteins. J Virol 91:e01488-16. https://doi.org/10.1128/JVI.01488-16.
46. Berger Rentsch M, Zimmer G. 2011. A vesicular stomatitis virus replicon-based bioassay for the rapid and sensitive determination of multi-species type I interferon. PLoS One 6:e25858. https://doi.org/10.1371/journal.pone.0025858.
47. Hoffmann M, Kruger N, Zmora P, Wrensch F, Herrler G, Pohlmann S. 2016. The hemagglutinin of bat-associated influenza viruses is activated by TMPRSS2 for pH-dependent entry into bat but not human cells. PLoS One 11:e0152134. https://doi.org/10.1371/journal.pone.0152134.
48. Schindelin J, Arganda-Carreras I, Frise E, Kaynig V, Longair M, Pietzsch T, Preibisch S, Rueden C, Saalfeld S, Schmid B, Tinevez JY, White DJ, Hartenstein V, Eliceiri K, Tomancak P, Cardona A. 2012. Fiji: an open-source platform for biological-image analysis. Nat Methods 9:676–682. https://doi.org/10.1038/nmeth.2019.
49. Livak KJ, Schmittgen TD. 2001. Analysis of relative gene expression data using real-time quantitative PCR and the 2(−Delta Delta C(T)) method. Methods 25:402–408. https://doi.org/10.1006/meth.2001.1262.
50. Guberina H, Witzke O, Timm J, Dittmer U, Muller MA, Drosten C, Bonin F. 2014. A patient with severe respiratory failure caused by novel human coronavirus. Infection 42:203–206. https://doi.org/10.1007/s15010-013-0509-9.
51. Drosten C, Seilmaier M, Corman VM, Hartmann W, Scheible G, Sack S, Guggemos W, Kallies R, Muth D, Junglen S, Muller MA, Haas W, Guberina H, Rohnisch T, Schmid-Wendtner M, Aldabbagh S, Dittmer U, Gold H, Graf P, Bonin F, Rambaut A, Wendtner CM. 2013. Clinical features and virological analysis of a case of Middle East respiratory syndrome coronavirus infection. Lancet Infect Dis 13:745–751. https://doi.org/10.1016/S1473-3099(13)70154-3.
52. ProMED. 2015. MERS-COV (31): Saudi Arabia, Germany ex United Arab Emirates, request for information. ProMED mail archive no. 20150308.3215456. http://www.promedmail.org/.